Approved for public release;
Distribution is unlimited.

ADA 284-736

Time Spread and Frequency Coherence in Acoustic Forward Scattering from the Sea Surface

by Peter H. Dahl and Azmi Al-Kurd

Accesion For
NTIS CRA&I ☑
DTIC T ☐
Unannounced ☐
Justification .....
By .....
Distribution /
Availability Codes
Dist | Avail and / or Special
A-1

Technical Report
APL-UW TR 9405
August 1994

Applied Physics Laboratory University of Washington
1013 NE 40th Street Seattle, Washington 98105-6698

SPAWAR N00039-88-C-0051
SPAWAR N00039-91-C-0072
ARL/PSU S89-2

Acknowledgments

The authors gratefully acknowledge the high-quality sea-state measurements made by Andrew Jessup and the many useful discussions with Jim Luby and Kevin Williams, all of APL-UW. The experimental work and data analysis were supported by the Office of Naval Technology (now ONR-T) Torpedo Environments Project managed by the Applied Research Laboratory at Pennsylvania State University (R. L. Culver, Project Leader).

ABSTRACT

Measurements of the characteristic time spread L (in seconds) of surface forward scattering were made from the research platform *FLIP* in January 1992. These data were compared with a model for L and matched the model to within an average relative error of 30%. The inverse, L^{-1} (in hertz), is a measure of the coherence bandwidth of the channel and therefore important in both designing waveforms and determining signal-processing strategies. Using the model for L, simulators can assess realistic magnitudes of the coherence bandwidth of the surface channel as a function of source/receiver geometry and environmental conditions.

Contents

List of Figures

EXECUTIVE SUMMARY

The Applied Physics Laboratory at the University of Washington (APL-UW) conducted forward-scattering measurements between 20 and 50 kHz from the research platform *FLIP* off the coast of California in January 1992. This work was sponsored by the Office of Naval Technology (now ONR-T) Torpedo Environments Program with technical management by the Applied Research Laboratory, Pennsylvania State University. The main objective was to obtain coordinated measurements of acoustic surface scattering, the subsurface bubble field, and the sea state in order to (1) understand more fully conditions imposed by the near-surface environment that affect the performance of torpedo guidance and control algorithms, and (2) improve high-frequency acoustic models used in designing, simulating, and predicting the performance of underwater weapon systems.

This report presents estimates of the characteristic time spread L (in seconds) in the surface forward scattering. The inverse, L^{-1} (in hertz), is a measure of the coherence bandwidth of the channel and therefore important in both designing waveforms and determining signal-processing strategies. The model provides a means to obtain realistic estimates of the coherence bandwidth for the channel as a function of both acquisition geometry and environment.

Fifty-eight estimates of L were made for frequencies between 20 and 50 kHz, ranges of 540–1000 m, grazing angles of 4.5°–17.6° and wind speeds from 0–8 m/s (16 knots). These estimates were compared with a model for L and matched the model to within an average relative error of ±30%. When the coherence bandwidth L^{-1} is estimated with the model, the relative error translates to approximately +40% and −20%.

The model for time spread is

$$L = \frac{2r_1 r_2}{r_1 + r_2} \frac{\tan^2 \gamma_0}{c} (1 - e^{-\theta/\gamma_0}) ,$$

where r_1 and r_2 are the incident and scattered slant ranges (in meters), respectively, along the specular path, c is the sound speed (in meters per second), and θ is the nominal grazing angle of the surface bounce path. The model requires a submodel for the rms slope $s = \tan \gamma_0$, where

$$\begin{aligned} s &= \sqrt{0.0046 \log_e(2.1U^2)} , \quad U \geq 1 \text{ m} \\ s &= 0.0584 , \quad U < 1 \text{ m} , \end{aligned}$$

and U is the wind speed (in meters per second) measured 10 m above the sea surface.

The coherence bandwidth estimates as determined by the time-spread estimates were also compared with a limited number of direct estimates of the frequency-coherence function. The latter, however, were encumbered by an interference between direct and surface-scattered paths and by an interference due to time delays between different frequency transmissions, both of which reduced the frequency-coherence function at a frequency separation of 60–80 Hz.

1. INTRODUCTION

This report presents results of an experiment to measure the characteristic time spread L (in seconds) in surface forward-scattered intensity at frequencies between 20 and 50 kHz. The inverse, L^{-1} (in hertz), is a measure of the width of the frequency-coherence function governing frequency-selective fading and is therefore important in both waveform design and signal-processing strategies. The estimates of L are compared to a model for L based on geometric variables (range, source and receiver depths, and surface grazing angle) and environmental variables (wind speed and rms sea slope). The model provides a means to obtain realistic estimates of the coherence bandwidth for the channel as a function of both acquisition geometry and environment.

The measurements were made from the research platform *FLIP* off the coast of California in January 1992. The objective was to obtain coordinated measurements of acoustic surface scattering, the subsurface bubble field, and the sea state. The measurements will be used to (1) understand more fully conditions imposed by the near-surface environment that affect the performance of torpedo guidance and control algorithms, and (2) improve high-frequency acoustic models used in the modeling and analysis of underwater weapon systems. Additional details on the experiment are given in Ref. 1, which also summarizes measurements of and a semiempirical model for the mean energy loss in surface-bounce paths due to extinction from near-surface bubbles.

Preliminary remarks and a summary of notation used in this report are given in Section 2. The experimental geometry and results of the time-spread analysis and environmental sea-state measurements are given in Section 3, along with model comparisons. Five signal suites were also amenable to estimation of the actual shape of the frequency-coherence function; although this data set is sparse, the results are included for comparison in Section 4. A discussion and summary are presented in Section 5.

2. PRELIMINARY REMARKS AND NOTATION

A brief summary of notation and usage is presented here. Further details on this subject are available in Refs. 2–5 and in the additional references cited below.

The scattering function $R_s(\tau, \phi)$ is a measure of the average delay, or time spread, (τ) and frequency spread (ϕ) that a transmitted signal will be subjected to by the channel (on an individual ping basis, this function is known as the spreading function and varies from ping to ping). For the forward-scattering measurements made from *FLIP*, the channel is defined as a single interaction with a time-varying random sea surface. Such a channel is usually time dispersive, because there are multipath arrivals leading to a spread of delays, and frequency dispersive, because the medium is time-varying, causing a broadening of the received signal spectrum (or Doppler spread). Both time and frequency dispersion render the channel doubly spread[6]; the property of angular dispersion adds yet another dimension of channel spreading.

In a manner analogous to the joint probability density function for two random variables, in this case τ and ϕ, one can define a marginal-scattering function for which one of the variables has been integrated out.[5] We define L (in seconds) as the characteristic width for a marginal-scattering function linked to time spread and B (in hertz) as the characteristic width for a marginal-scattering function linked to frequency spread. More precisely, we can define L and B as the square root of the second moment of their respective marginal-scattering functions. Under some conditions, the scattering function may be separable[7] such that

$$R_s(\tau, \phi) = R_\tau(\tau) R_\phi(\phi) \ , \tag{1}$$

where $R_\tau(\tau)$ is the so-called delay, or time-spread, profile and $R_\phi(\phi)$ is the Doppler, or frequency-spread, profile.

If scattering from the sea surface is incoherent, then the intensity time-spread function and frequency-coherence function are related by Fourier transforms.[8] Accordingly, the inverse, L^{-1} (in hertz), is an approximate measure of the coherence bandwidth of the channel. In other words, transmitting signals with a bandwidth $W > L^{-1}$ may result in frequency-selective fading, while for $W < L^{-1}$ all frequencies behave more or less the same in terms of fading statistics.

For completeness, an estimate for B can be derived using[9]

$$B = 0.128 U f \sin\theta \ , \tag{2}$$

where f is the frequency in kilohertz, U is the wind speed in meters per second measured 10 m above the sea surface, and θ is the sea-surface grazing angle. Based on Eq. (2), B is approximately 5 Hz for the range of grazing angles, wind speeds, and frequencies that apply to the FLIP forward-scattering measurements.

3. EXPERIMENTAL GEOMETRY, TIME-SPREAD MEASUREMENTS, SEA-SLOPE COMPUTATIONS, AND MODEL COMPARISONS

The geometry used to measure the time spread in surface forward-scattered intensity is shown in Figure 1. Signals were transmitted from one of three ITC-1032 transducers suspended at depths of 27, 57, and 147 m from the spar buoy. The spar buoy was tethered to *FLIP* by a 1000-m-long cable and ranged from 500 to 1000 m from the vessel. The receiver options at *FLIP* consisted of the ITC-1032 transducer located on the tip of the 12-m-long subsurface boom attached to *FLIP*'s hull at a depth of 28.5 m, the line array, and the Mk-46 array. Both arrays were attached to *FLIP*'s hull at a depth of 66 m.

Frequency spectra for sea-surface displacement $S_{\eta\eta}(f)$, made with a vertical-incidence scatterometer, were taken every 20 minutes by A. Jessup of APL-UW. From the displacement spectra, we computed a large-scale mean-square surface slope ($s^2_{\mathcal{W}}$) using

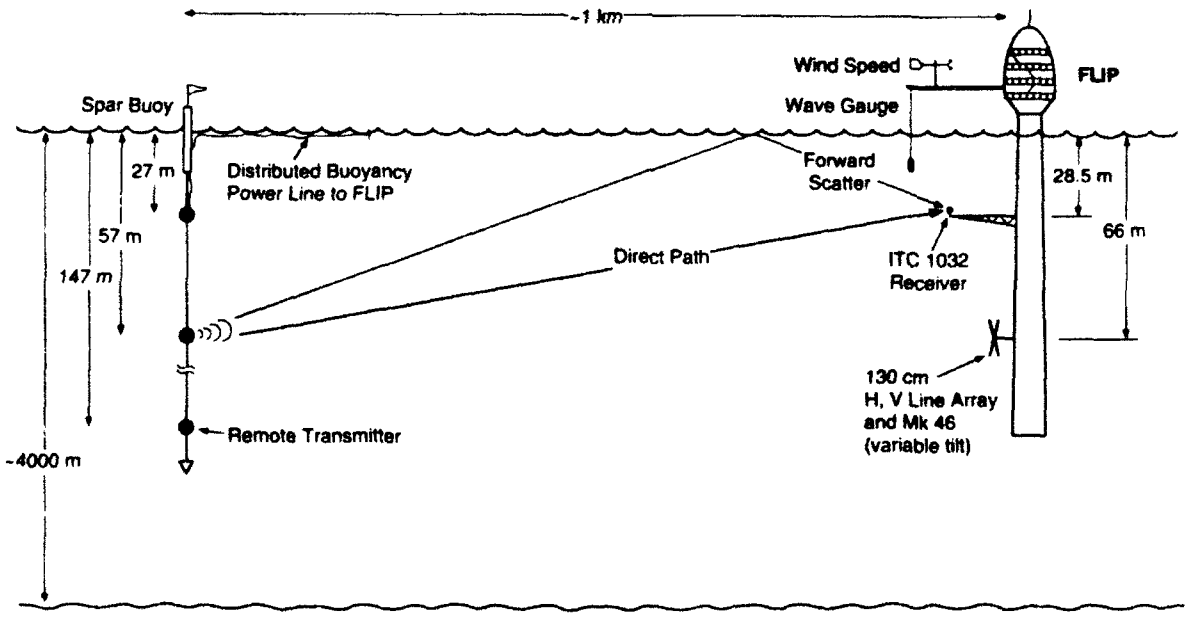

Figure 1. Experimental geometry for measurements of time spread and frequency coherence in surface forward scattering. Measurements were made using all three sources suspended from the spar buoy and all three receiver systems attached to FLIPs hull. The spar's buoy range varied between 500 and 1000 m.

$$s_W^2 = \frac{(2\pi)^4}{g^2} \int_0^{f_c} f^4 S_{\eta\eta}(f) df \ , \tag{3}$$

where g is a gravitational constant and f_c is the integration cutoff frequency. For a sea-surface wavenumber spectrum, numerical simulations by McDaniel[10] suggest setting a wavenumber cutoff equal to 0.4 times the magnitude of the acoustic wavenumber k. Upon using the deep-water dispersion relation, this gives f_c equal to $\sqrt{(0.4gk)}/2\pi$. The spot size of the scatterometer prevents frequencies $\gtrsim$ 0.6 Hz from being adequately resolved. To correct for this, an f^{-5} tail is appended to $S_{\eta\eta}$ for frequencies $>$ 0.6 Hz.[11] The rms slope s_W, significant wave height (SWH), and wind speed for each acoustic measurement are listed in Table 1. Additional details on the environmental measurements are discussed in Refs. 1 and 12.

We estimate L in the following manner. A model[13] for the intensity impulse response is numerically convolved with the particular transmit pulse envelope used in the *FLIP* measurements (typically 1–8 ms cw). The result gives a model for the time dependence of surface-scattered intensity which includes L as a free parameter. We then estimate L by matching this model with ensemble-averaged data in a least squares sense, such as in the example shown in Figure 2 where L = 3 ms. Results for 58 such estimates made for frequencies between 20 and 50 kHz, ranges of 500–1000 m, grazing angles of 7°–18°, and wind speeds of 0–8 m/s are listed in Table 1. In the table, SD = source depth, RD = receiver depth, and T = pulse length. The variables s_A and L_{MOD} are discussed in the next section.

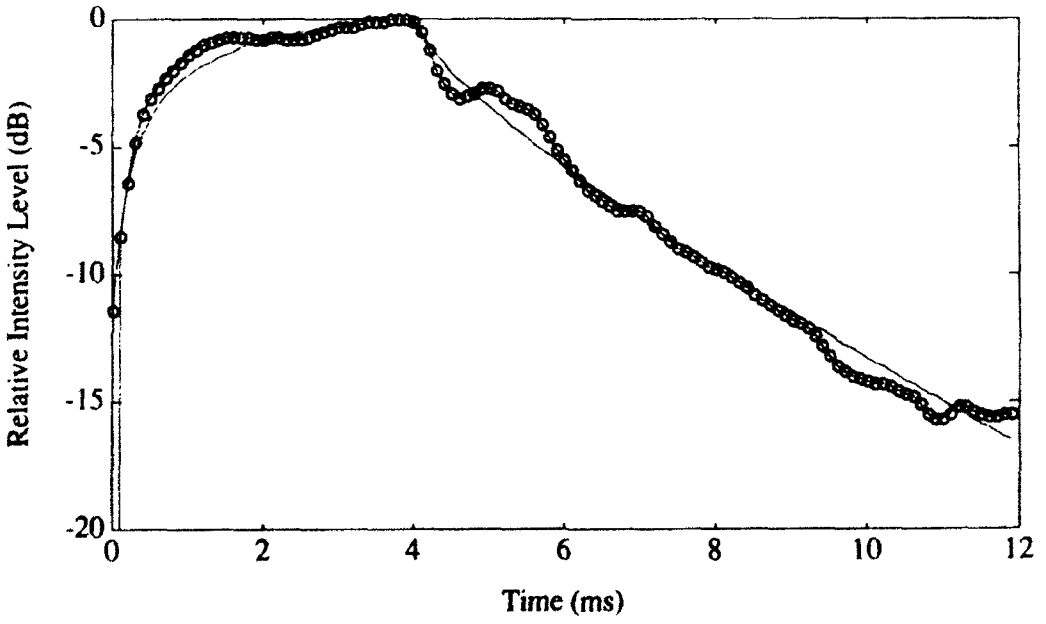

Figure 2. Model for the time dependence of surface-scattered intensity (thin line) fitted to data (circles) using L = 3 ms.

Table 1. Summary of time-spread database derived from FLIP experiment.

RUN ID	FREQ (kHz)	RANGE (m)	SD (m)	RD (m)	θ (deg)	T (ms)	WIND (m/s)	SWH (m)	s_W (radians)	s_A (radians)	L (ms)	L_{MOD} (ms)
SBL109	20	874	147	28	10 9	4	8	1 5	0 11	0 13	2	2 6
SBL109	30	874	147	28	10 9	4	8	1 5	0 12	0 13	2	2 6
SBL110	20	874	147	28	10 9	4	7 8	1 5	0 11	0 15	3	2 6
SBL110	30	874	147	28	10 9	4	7 8	1 5	0 12	0 15	3	2 6
SBL110	40	874	147	28	10 9	4	7 8	1 5	0 12	0 15	3	2 6
SBL111	20	855	27	28	4 5	4	7 8	1 5	0 12	0 11	1 7	2 6
SBL111	50	855	27	28	4 5	4	7 8	1 5	0 13	0 1	1 6	2 6
SBL114	30	995	147	28	11 1	4	7	1 9	0 12	0 14	2 6	2 8
SBL114	40	995	147	28	11 1	4	7	1 9	0 12	0 14	2 6	2 8
SBL115	20	995	147	28	11 1	4	5 3	2	0 1	0 11	1 8	2 6
SBL115	30	995	147	28	11 1	4	5 3	2	0 1	0 11	1 7	2 6
SBL115	40	995	147	28	11 1	4	5 3	2	0 11	0 11	1 7	2 6
SBL115	50	995	147	28	11 1	4	5 3	2	0 11	0 11	1 8	2 6
SBL116	20	540	147	28	17 6	4	4 1	1 3	0 09	0 14	1 8	1 5
SBL116	30	540	147	28	17 6	4	4 1	1 3	0 09	0 14	1 8	1 5
SBL116	40	540	147	28	17 6	4	4 1	1 3	0 1	0 14	1 8	1 5
SBL116	50	540	147	28	17 6	4	4 1	1 3	0 1	0 14	1 8	1 5
SBL117	20	540	147	28	17 6	8	4 1	1 3	0 09	0 15	2	1 5
SBL117	20	540	147	28	17 6	8	4 1	1 3	0 09	0 15	2	1 5
SBL117	20	540	147	28	17 6	8	4 1	1 3	0 1	0 15	2	1 5
SBL117	20	540	147	28	17 6	8	4 1	1 3	0 1	0 15	2	1 5
SBL119	20	669	147	28	14 6	4	0	1 1	0 06	0 06	0 4	0 4
SBL119	30	669	147	28	14 6	4	0	1 1	0 06	0 05	0 3	0 4
SBL119	40	669	147	28	14 6	4	0	1 1	0 06	0 06	0 5	0 4
SBL119	50	669	147	28	14 6	4	0	1 1	0 06	0 06	0 5	0 4
SBL133	20	668	147	28	14 3	1	4 3	1 8	0 08	0 08	0 8	1 8
SBL133	30	668	147	28	14 3	1	4 3	1 8	0 08	0 1	1 2	1 8
SBL133	40	668	147	28	14 3	1	4 3	1 8	0 09	0 1	1 2	1 8
SBL133	50	668	147	28	14 3	1	4 3	1 8	0 09	0 1	1 2	1 8
SBL134	20	701	147	28	14	1	2 9	1 6	0 08	0 08	0 8	1 5
SBL134	30	701	147	28	14	1	2 9	1 6	0 08	0 08	0 8	1 5
SBL134	40	701	147	28	14	1	2 9	1 6	0 08	0 08	0 8	1 5
SBL134	50	701	147	28	14	1	2 9	1 6	0 08	0 08	0 8	1 5
SBL135	20	701	147	28	7 2	1	2 9	1 6	0 08	0 07	0 5	1 1
SBL135	30	701	147	28	7 2	1	2 9	1 6	0 08	0 07	0 5	1 1
SBL135	40	701	147	28	7 2	1	2 9	1 6	0 08	0 07	0 5	1 1
SBL135	50	701	147	28	7 2	1	2 9	1 6	0 08	0 07	0 5	1 1
SBL138	20	666	147	28	14 5	4	4 4	2 1	0 09	0 1	1 2	1 8
SBL138	30	666	147	28	14 5	4	4 4	2 1	0 09	0 09	1	1 8
SBL138	40	666	147	28	14 5	4	4 4	2 1	0 1	0 15	2 3	1 8
SBL138	50	666	147	28	14 5	4	4 4	2 1	0 1	0 15	2 3	1 8
LAE102	30	1000	147	66	12	4	7 6	1 8	0 1	0 12	3 5	4 9
LAE103	30	1000	147	66	12	8	7 6	1 8	0 1	0 12	3 5	4 9
LAE104	20	1000	147	66	12	8	7 6	1 8	0 09	0 12	3 3	4 9
LAE105	40	1000	147	66	12	8	7 6	1 8	0 1	0 15	5	4 9
LAE107	30	1000	147	66	12	8	7 6	1 8	0 1	0 12	3 4	4 9
LAE109	30	1000	57	66	7	4	5 3	2	0 1	0 09	2	3 7
LAE110	20	576	147	66	20	12	3 2	2	0 1	0 12	2 5	2 3
LAE110	30	576	147	66	20	12	3 2	2	0 1	0 11	2	2 3
LAE110	40	576	147	66	20	12	3 2	2	0 11	0 11	2	2 3
LAE112	30	750	147	66	15	10	0 5	1 5	0 06	0 07	1 2	0 8
LAE115	40	723	147	66	16	10	0 5	1 5	0 06	0 03	0 2	0 7
LAE117	30	1000	147	66	12	8	4 6	2 1	0 09	0 11	3	4 1
FWD46_104	25	678	57	66	10	10	3 1	1 3	0 09	0 08	1 2	2 4
FWD46_108	30	1000	91	66	9	10	4 6	2 1	0 1	0 07	1 5	4
FWD46_109	30	1000	91	66	9	10	4 6	2 1	0 1	0 08	1 8	4
FWD46_110	30	1000	91	66	9	10	4 6	2 1	0 1	0 07	1 5	4
FWD46_111	30	1000	91	66	9	10	4 6	2 1	0 1	0 08	2	4

4. MODEL VS DATA COMPARISONS

A model for the characteristic time spread L in forward scatter is[13,14]

$$L = \frac{2r_1 r_2}{r_1 + r_2} \frac{\tan^2 \gamma_0}{c} (1 - e^{-\theta/\gamma_0}) , \tag{4}$$

where r_1 and r_2 are the incident and scattered slant ranges (in meters), respectively, along the specular path, c is the nominal sound speed (in meters per second), and θ is the nominal grazing angle of the surface bounce path. This model requires a submodel for the rms slope $s = \tan \gamma_0$. For this, we use a model based on a logarithmic fit[15] of the classic set of optical glitter measurements by Cox and Munk* of the mean square slope for a slick-covered surface,

$$\begin{aligned} s &= \sqrt{0.0046 \log_e(2.1U^2)} , \quad U \geq 1 \text{ m} \\ s &= 0.0584 , \qquad\qquad\quad U < 1 \text{ m} . \end{aligned} \tag{5}$$

The logarithmic wind speed dependence in Eq. (5) from Ref. 15 is restricted to wind speeds $U \geq 1$ m/s. For wind speeds less than 1 m/s, we set s equal to 0.0584 (equivalent to Eq. (5) evaluated at 1 m/s) because data on sea surface slope for extremely low wind speeds are too scattered to specify a more precise functional form.

The time spreads L_{MOD} predicted using the model in Eq. (4) and the submodel in Eq. (5) are given alongside each measured time spread L in Table 1. The predictions have a relative uncertainty of approximately ±30%. The rms value of the model (L_{MOD}) minus data (L) vectors is 0.75 ms. We conclude that Eq. (4), along with the submodel for rms sea slope, enables one to assess realistic magnitudes of the coherence bandwidth (defined as L^{-1}) as a function of both acquisition geometry (r_1, r_2, and θ) and environment (U). The relative uncertainty in L translates to approximately +40% and −20% for coherence bandwidth predictions.

We can also infer an estimate of the large-scale sea slope s from the original measurements of L and the geometric variables listed in Table 1. To do this, Eq. (4) is solved numerically using the Newton-Raphson method[16] to find the unknown γ_0. The sea-slope estimates (equal to $\tan \gamma_0$) derived from the acoustic estimates of time spread are referred to as s_A in Table 1 and are plotted vs wind speed in Figure 3 along with s_W and s computed using Eq. (5). The scatter shown in Figure 3 is quite typical of slope-vs-wind-speed data. The model for s based on the Cox and Munk

*The slope measurements by Cox and Munk were made in both clean water surface conditions and oil-slick-covered surface conditions. The effect of the oil slick was to effectively damp out surface waves with a wavelength less than about 30 cm. Therefore we use the slick-covered measurements because they are more representative of slope conditions sampled by finite acoustic wavelengths.

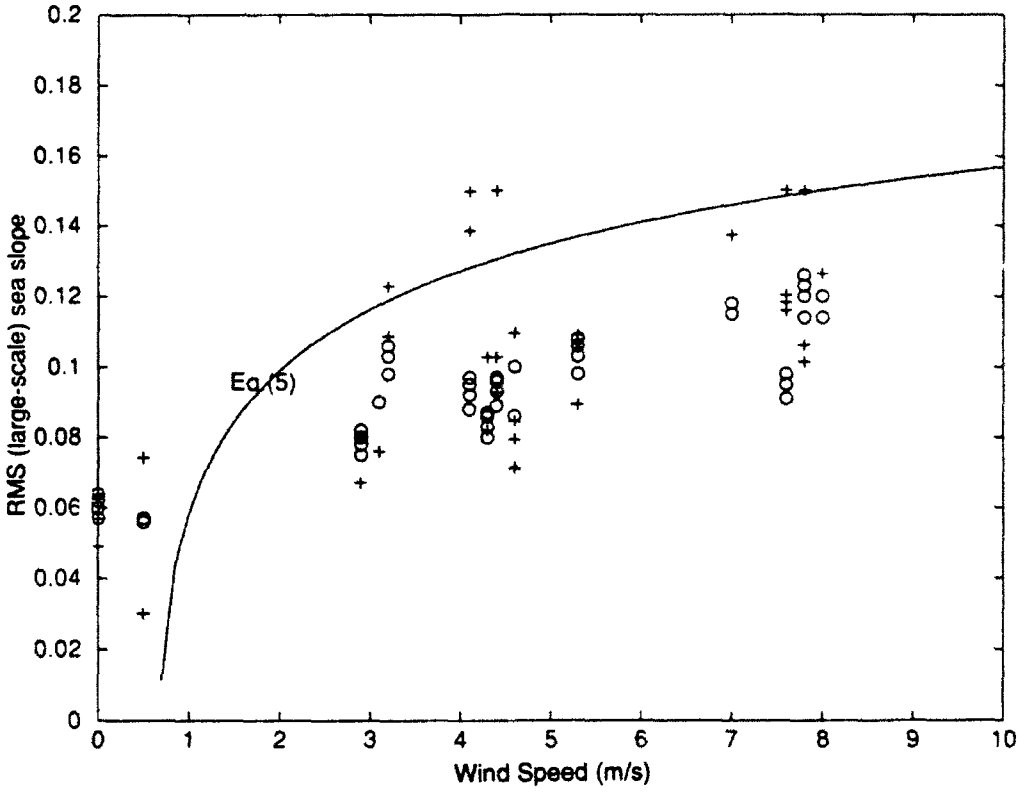

Figure 3. Model for rms large-scale sea slope, Eq. (5), vs slope estimates derived from the time-spread database and inversion of Eq. (4) (+) and slope estimates derived from wave-gauge data and Eq. (3) (o).

data, Eq.(5), describes the s_A data reasonably well and tends to form an upper bound to the s_W data. Recall that the s_W estimates depend on an integration cutoff that increases with acoustic frequency. Thus the multifrequency runs (20, 30, 40, and 50 kHz) listed in Table 1 will show up as a clustering of points in Figure 3, with the highest frequency giving a slightly higher estimate of s_W. Furthermore the f^{-5} tail, appended to $S_{\eta\eta}$ for frequencies >0.6 Hz, influences the integral in Eq. (3). A tail of f^{-4}, for example, would increase the final estimates for s_W^2 as derived from Eq. (3).

5. FREQUENCY COHERENCE FUNCTION ESTIMATES

Estimates of the frequency-coherence function for forward scattering were made using signal suites specified by Dr. D. Ricker of ARL-PSU; these suites are referred to as Arctic, Costas-1, and Costas-2. The received data from the Arctic pulse are stored in a file called FWDmk46.101. The original (transmitted) pulse is 560 ms long and constitutes seven frequency chips, with each chip having a different frequency offset from the carrier frequency. The received data from the Costas-1 pulse are stored in the file FWDmk46.102. The original pulse is 500 ms long and divided into three periods; the first 200 ms contains 27 frequency chips, the following 100 ms is silence, and the last 200 ms contains 27 frequency chips. The received data from the Costas-2 pulse are stored in the files FWDmk46.103 and FWDmk46.105. Each of the above files consists of 25 pings recorded on four channels. For the Costas-1 and Costas-2 pulses, the received signal is split into two parts (see Table 2) because of the 100-ms silence between the two transmitted waveforms; each part is the channel response to waveform A, B, or C. The offset frequencies for the various chips used in waveform A are listed in Table 3. Waveform B is the same as A with the sign reversed; waveform C is a 200-ms cw pulse with zero offset from the carrier frequency.

Table 2. Pulse shapes for Costas-1 and Costas-2 waveforms.

Signal Name	Duration (ms)	Shape
Costas-1	500 ms	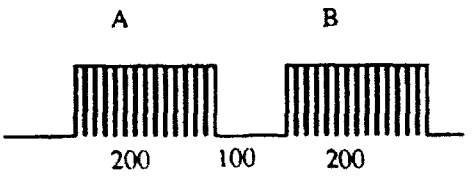
Costas-2	500 ms	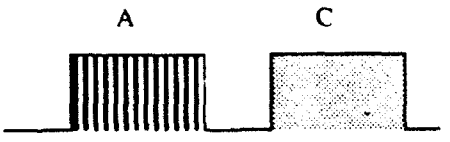

Frequency (Hz)
-498.1
-273.1
-203.8
-411.5
-376.9
-290.4
-134.6
-359.6
-550
-446.2
-117.3
-186.5
-325
-307.7
-342.3
-221.2
-169.2
-515.4
-151.9
-463.5
-255.8
-428.8
-532.7
-100
-394.2
-480.8
-238.5

Table 3.

Offset frequency for the 27 chips in Costas waveform A. The actual transmitted frequency equals a carrier frequency plus that shown in the table. The order of chip transmission is shown from top to bottom; e.g., the first entry (−498.1 Hz) was the first chip to be transmitted.

The received signal is processed through a filter bank, where the transfer function of each cell is weighted with a Hanning window with a central frequency and width equal to those of the corresponding frequency chip. Each filter-bank output is cross correlated with every other output. The coherence between the responses of two frequency chips is defined as

$$\gamma_{ij}(\tau) = \frac{\langle y_{f_i}(t) y^*_{f_j}(t) \rangle}{\sqrt{\langle |y_{f_i}(t)|^2 \rangle \langle |y_{f_j}(t)|^2 \rangle}}, \tag{6}$$

where f_i and f_j are the central frequencies of the i^{th} and the j^{th} chips, and $y_{f_i}(t)$ is the output of the i^{th} cell of the filter bank. The coherence magnitude corresponds to $|\gamma_{ij}(\tau = 0)|$ and indicates the amount of coherence between the chip centered at

frequency f_i and that centered at frequency f_j. The final result is an $N \times N$ matrix of $|\gamma_{ij}(\tau = 0)|$, where N is the number of chips; an example is shown in Figure 4.

The chips can be ordered, or numbered, by their frequency offset or by their time of transmission within the waveform. In Figure 4 the bottom and left axes show the chip numbers according to offset frequency sequencing, and the top and right axes show the chip numbers according to the transmission time sequencing. For example, the chip with an offset frequency of -151.9 Hz, has a frequency sequence number of 24 and a time sequence number of 19 (Table 3). The best coherence is achievable when chips are close in both frequency and time, e.g., two chips that are close in frequency but far apart in time will still show weak coherence. For example, in Figure 4 the neighboring frequency chips 4 (-498.1 Hz) and 5 (-480.8 Hz) show weak coherence because they were transmitted far apart in time.

Figure 4 summarizes all the coherence estimates for one run, but it is admittedly difficult to interpret. A simpler view is shown in Figures 5–9 which show the coherence of pairs of temporally neighboring chips as a function of their frequency separation. Note that the analysis was performed using the ensemble average (25 pings) for one quad and for the coherent sum of four quads of the Mk 46 array, and no significant difference was observed in the results.

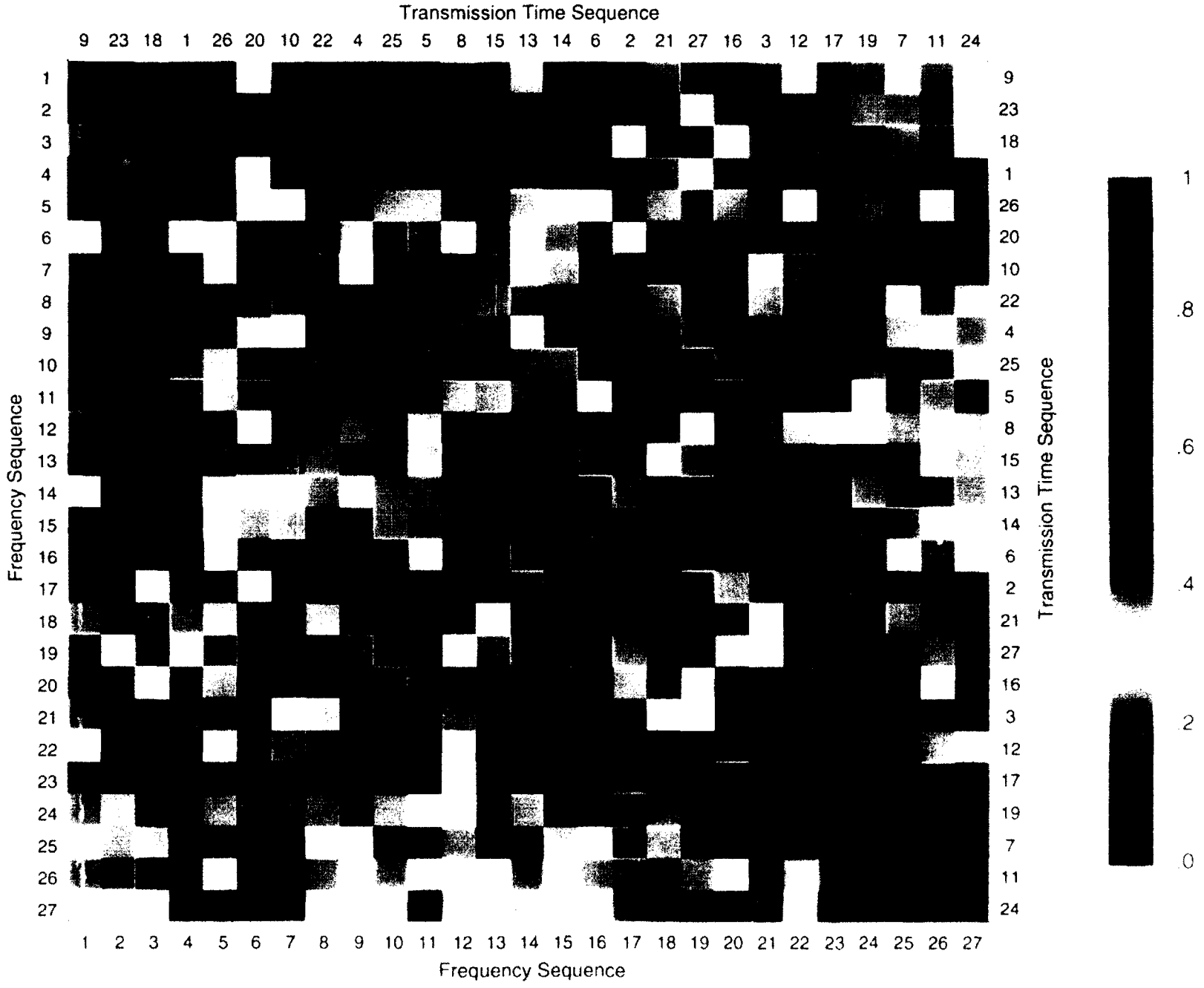

Figure 4. Frequency coherence matrix of channel response to the transmitted signal (Costas-2, waveform A). The lower and left axes show the chip number by its frequency sequence; the top and right axes show the chip number by its transmission-time sequence.

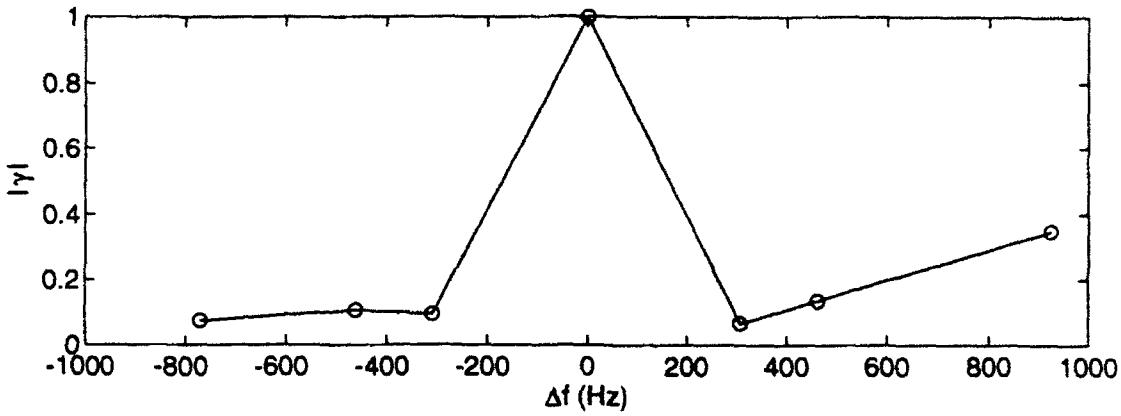

Figure 5. Magnitude of frequency coherence vs frequency difference Δf based on temporally neighboring chips for file FWDmk46.101 and pulse type Arctic.

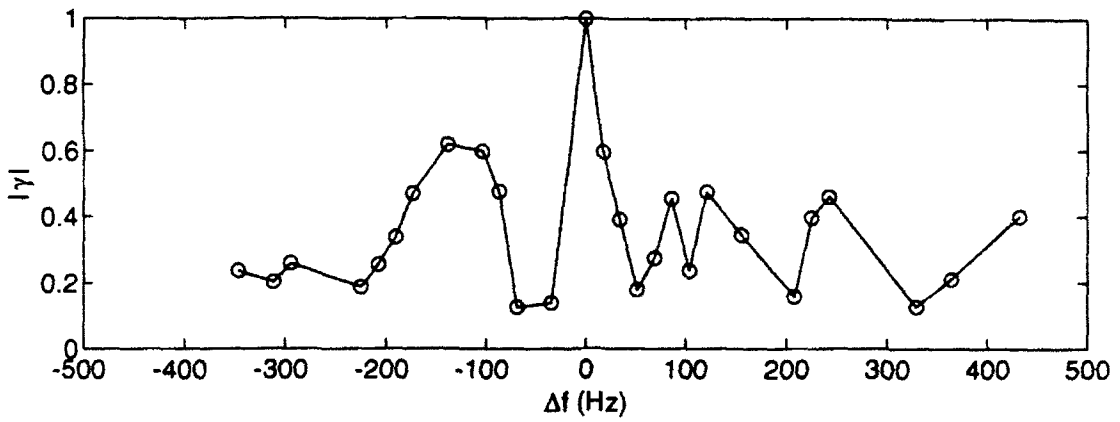

Figure 6. Magnitude of frequency coherence vs frequency difference Δf based on temporally neighboring chips for file FWDmk46.102 and pulse type Costas-1 A.

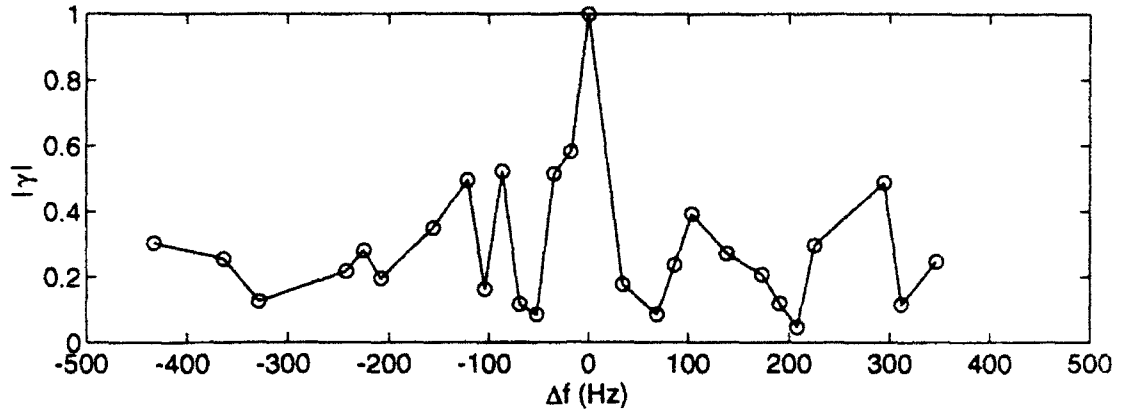

Figure 7. Magnitude of frequency coherence vs frequency difference Δf based on temporally neighboring chips for file FWDmk46.102 and pulse type Costas-1 B.

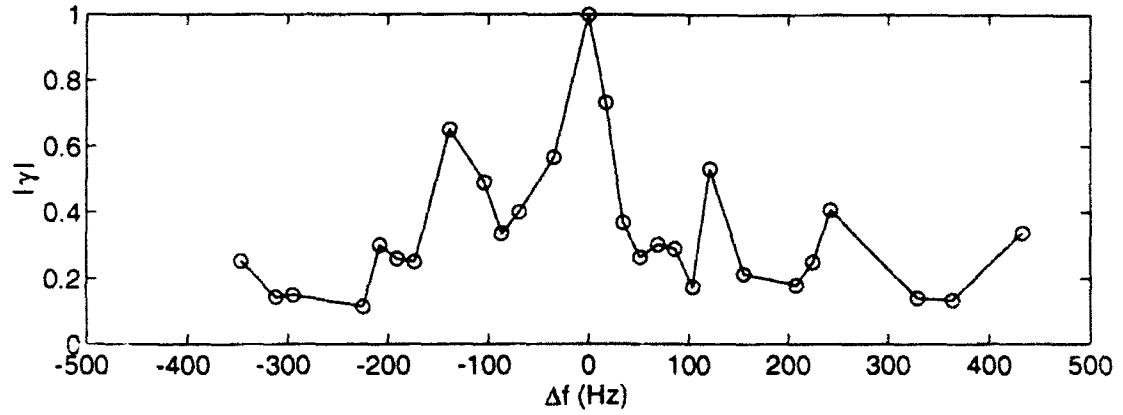

Figure 8. Magnitude of frequency coherence vs frequency difference Δf based on temporally neighboring chips for file FWDmk46.103 and pulse type Costas-2 A.

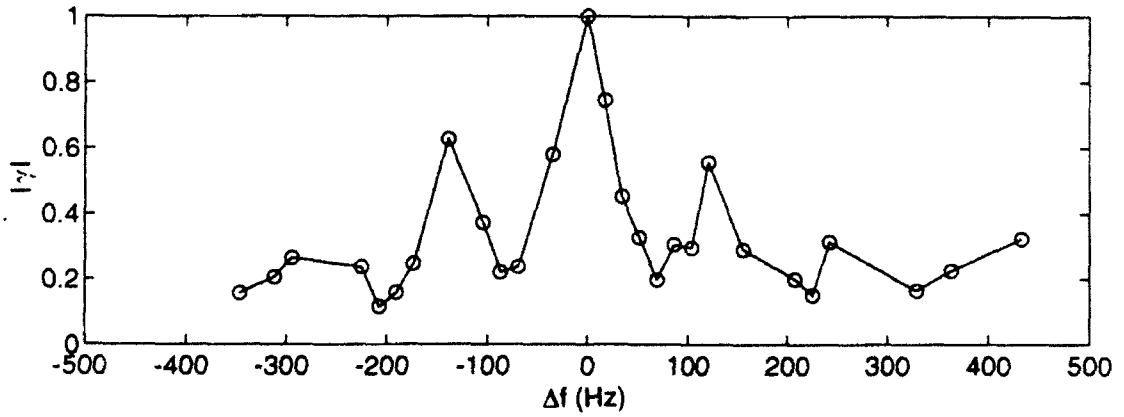

Figure 9. Magnitude of frequency coherence vs frequency difference Δf based on temporally neighboring chips for file FWDmk46.105 and pulse type Costas-2 A.

6. DISCUSSION AND SUMMARY

The acoustic runs for which the frequency coherence was estimated and shown in Figures 5–9 were taken within 1 hour of each other. The source and receiver depths were 57 and 66 m, respectively; the range was 676 m, the grazing angle 10°, and the wind speed 4 m/s. Using these variables in Eqs. (4) and (5), we would expect the time spread L to be about 2.5 ms and therefore the coherence bandwidth to be about 400 Hz. The coherence bandwidth estimated from Figures 5–9 is clearly less than 400 Hz, more on the order of 50 Hz (full bandwidth).

A probable reason for this difference is that, for these runs, we were unable to effectively separate the direct path from the surface-reflected path which arrived ~7 ms later. Thus the frequency-coherence functions shown in Figures 5–9 suffer from interference between the direct and surface-bounce paths (although the frequency spacing in Figure 5 is not small enough to show this). Note also that there is a time delay of 7.5 ms between neighboring frequency chips within the Costas waveforms used for the coherence estimates in Figures 6–9. The combination of direct and surface interference and the time delay between neighboring frequency chips significantly reduces the coherence for frequency differences Δf satisfying relation $|\Delta f|\Delta T \approx 0.5$, where ΔT is either the travel-time difference or the chip time delay. Frequency differences $|\Delta f|$ in the neighborhood of 60 to 80 Hz meet this criterion, with this effect shown in an approximate sense in Figures 6–9 (though less clearly in Figure 7). Note, however, that in these same figures the coherence rises for $|\Delta f|$ sufficiently greater than about 80 Hz but less than about 200 Hz. This is reasonably consistent with a coherence full bandwidth of ~400 Hz, as predicted by the time-spread estimates.

In summary, our main findings pertain to the parameter L, defined as the characteristic time spread, in seconds, in the surface forward-scattered intensity. The 58 estimates of L were compared with predicted values based on a model, Eqs. (4) and (5), and the model matched the data within a relative uncertainty of ±30%. The inverse, L^{-1} (in hertz), is an approximate measure of the coherence bandwidth of the channel. Using the model for L, simulators can assess realistic magnitudes of the surface-channel coherence bandwidth as a function of source/receiver geometry and environmental conditions.

We were unable to match estimates of the frequency coherence function with the time-spread data because of interference between direct and surface-bounce paths and interference due to time delays between different frequency transmissions, both of which reduced the magnitude of the frequency-coherence function for $|\Delta f|$ in the range 60–80 Hz. Coherence properties away from this range were reasonably consistent with the expected coherence bandwidth based on the time-spread measurements.

REFERENCES

1. P. H. Dahl, "Bubble Attenuation Effects in High-Frequency Surface Forward Scattering Measurements from *FLIP*," APL-UW TR 9307, Applied Physics Laboratory, University of Washington, May 1993.
2. R. S. Kennedy, *Fading Dispersive Communication Channels*, Wiley-Interscience, New York, 1969.
3. H. L. Van Trees, *Detection, Estimation and Modulation Theory*, Vol. III, Wiley, New York, 1971.
4. J. G. Proakis, *Digital Communications*, McGraw-Hill, New York, 1983.
5. L. J. Ziomek, *Underwater Acoustics: A Linear Systems Theory Approach*, Academic Press, New York, 1985.
6. W. C. Knight, R. G. Pridham, and S. M. Kay, "Digital signal processing for sonar," *Proc. IEEE, 69*, 1451–1506, 1981.
7. J. Johnsen, "Spectrum analysis of reverberations," in *Signal Processing*, J. W. R. Griffiths, P. L. Stocklin, and C. Van Schooneveld, Eds., Academic Press, New York, 1973, pp. 97–115.
8. M. H. Brill, X. Zabal, and S. L. Adams, "Time spread of acoustic signals reflecting from a fixed rough boundary," *J. Acoust. Soc. Am., 75*, 1062–1070, 1984.
9. R. L. Swarts and C. J. Eggen, "Simplified model of the spectral characterization of high-frequency surface scatter," *J. Acoust. Soc. Am., 59*, 846–581, 1976.
10. S. T. McDaniel, "Models for Predicting Bistatic Surface Scattering Strength," TM90-88, Applied Research Laboratory, Pennsylvania State University, March 1990.
11. M. L. Banner, "Equilibrium spectra of wind waves," *J. Phys. Oceanogr., 20*, 966–984, 1990.
12. P. H. Dahl and A. T. Jessup, "Bubble Plumes and Breaking Waves: Measurements from R/P *FLIP*, January 1992," APL-UW TM 2-92, Applied Physics Laboratory, University of Washington, May 1992.
13. E. I. Thorsos, "Surface Forward Scattering and Reflection," APL-UW 7-83, Applied Physics Laboratory, University of Washington, May 1984.
14. J. F. McDonald and F. B. Tuteur, "Calculation of the range-Doppler plot for a doubly spread surface-scatter channel at high Rayleigh parameters," *J. Acoust. Soc. Am., 57*, 1025–1029, 1975.

15. O. M. Phillips, *The Dynamics of the Upper Ocean* Cambridge University Press. Cambridge, 1977.

16. F. B. Hildebrand, *Advanced Calculus for Applications*, Prentice-Hall, Englewood Cliffs, New Jersey, 1976.

REPORT DOCUMENTATION PAGE

Form Approved
OPM No. 0704-0188

Public reporting burden for this collection of information is estimated to average 1 hour per response, including the time for reviewing instructions, searching existing data sources, gathering and maintaining the data needed, and reviewing the collection of information. Send comments regarding this burden estimate or any other aspect of this collection of information, including suggestions for reducing this burden, to Washington Headquarters Services, Directorate for Information Operations and Reports, 1215 Jefferson Davis Highway, Suite 1204, Arlington, VA 22202-4302, and to the Office of Information and Regulatory Affairs, Office of Management and Budget, Washington, DC 20503.

1. AGENCY USE ONLY *(Leave blank)*	2. REPORT DATE	3. REPORT TYPE AND DATES COVERED
	August 1994	Technical

4. TITLE AND SUBTITLE
Time Spread and Frequency Coherence in Acoustic Forward Scattering from the Sea Surface

5. FUNDING NUMBERS
SPAWAR Contract N00039-88-C-0051
SPAWAR Contract N00039-91-C-0072
ARL/PSU S89-2

6. AUTHOR(S)
Peter H. Dahl and Azmi Al-Kurd

7. PERFORMING ORGANIZATION NAME(S) AND ADDRESS(ES)
Applied Physics Laboratory
University of Washington
1013 NE 40th Street
Seattle, WA 98105-6698

8. PERFORMING ORGANIZATION REPORT NUMBER
APL-UW TR 9405

9. SPONSORING / MONITORING AGENCY NAME(S) AND ADDRESS(ES)
Applied Research Laboratory
The Pennsylvania State University
P.O. Box 30
State College, PA 16804
Attn: Lee Culver

10. SPONSORING / MONITORING AGENCY REPORT NUMBER

11. SUPPLEMENTARY NOTES

12a. DISTRIBUTION / AVAILABILITY STATEMENT
Approved for public release. Distribution is unlimited.

12b. DISTRIBUTION CODE

13. ABSTRACT *(Maximum 200 words)*

Measurements of the characteristic time spread L (in seconds) of surface forward scattering were made from the research platform *FLIP* in January 1992. These data were compared with a model for L and matched the model to within an average relative error of 30%. The inverse, L^{-1} (in hertz), is a measure of the coherence bandwidth of the channel and therefore important in both designing waveforms and determining signal-processing strategies. Using the model for L, simulators can assess realistic magnitudes of the coherence bandwidth of the surface channel as a function of source/receiver geometry and environmental conditions.

14. SUBJECT TERMS
Time spread, frequency coherence, sea surface slope, environmental acoustics

15. NUMBER OF PAGES
23

16. PRICE CODE

17. SECURITY CLASSIFICATION OF REPORT	18. SECURITY CLASSIFICATION OF THIS PAGE	19. SECURITY CLASSIFICATION OF ABSTRACT	20. LIMITATION OF ABSTRACT
Unclassified	Unclassified	Unclassified	SAR